Faraday Discussions

Accepted Manuscript

This manuscript will be presented and discussed at a forthcoming Faraday Discussion meeting. All delegates can contribute to the discussion which will be included in the final volume.

Register now to attend! Full details of all upcoming meetings: http://rsc.li/fd-upcoming-meetings

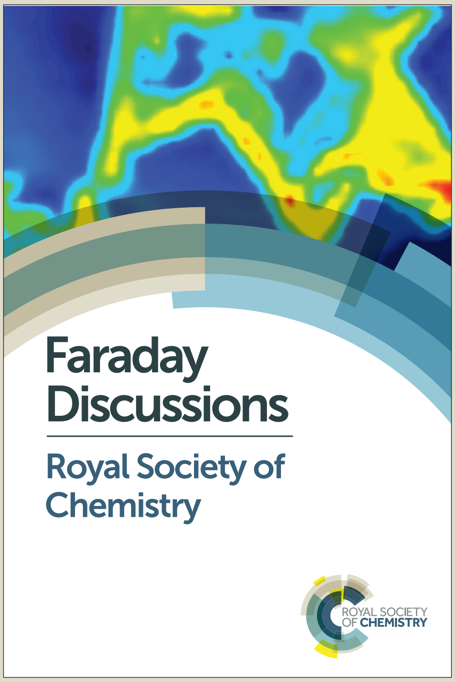

Faraday Discussions

Royal Society of Chemistry

This is an *Accepted Manuscript*, which has been through the Royal Society of Chemistry peer review process and has been accepted for publication.

Accepted Manuscripts are published online shortly after acceptance, before technical editing, formatting and proof reading. Using this free service, authors can make their results available to the community, in citable form, before we publish the edited article. We will replace this *Accepted Manuscript* with the edited and formatted *Advance Article* as soon as it is available.

You can find more information about *Accepted Manuscripts* in the Information for Authors.

Please note that technical editing may introduce minor changes to the text and/or graphics, which may alter content. The journal's standard Terms & Conditions and the Ethical guidelines still apply. In no event shall the Royal Society of Chemistry be held responsible for any errors or omissions in this *Accepted Manuscript* or any consequences arising from the use of any information it contains.

ROYAL SOCIETY OF CHEMISTRY

www.rsc.org/faraday_d

Journal Name

ARTICLE

Single-molecule spectromicroscopy: a route towards sub-wavelength refractometry

Received 00th January 20xx,
Accepted 00th January 20xx

DOI: 10.1039/x0xx00000x

www.rsc.org/

T. A. Anikushina,[a] M. G. Gladush,[a] A. A. Gorshelev,[a] and A. V. Naumov[a,b,*]

We suggest a novel approach for spatially resolved probing of local fluctuations of the refractive index *n* in solids by means of single-molecule (SM) spectroscopy. It is based on the dependence $T_1(n)$ of the effective radiative lifetime T_1 of dye centres in solids on *n* due to the local-field effects. Detection of SM zerophonon lines at low temperatures gives the values of SM natural spectral linewidth (which is inverse proportional to T_1) and makes it possible to reveal the distribution of the local *n* values in solids. Here we demonstrate this possibility on the example of amorphous polyethylene and polycrystalline naphthalene doped with terrylene. Particularly, we show that the obtained distributions of lifetime limited spectral linewidths of terrylene molecules embedded into these matrices are due to the spatial fluctuations of the refractive index local values.

1. Introduction

One of the most important characteristics of a material that determine many of its macroscopic properties is the refractive index *n*. It is included as a parameter in classical equations (e.g., Fresnel's and Maxwell's), linked to dielectric permitivity and magnetic permeability, and known to depend on temperature, pressure and wavelength [1]. In recent years a special attention has been attracted to the refractive index in relation to metamaterials, which are assumed to have the negative *n* [2, 3].

Since Ernst Abbe invented the refractometer in 1874 [4] the most precise techniques for measuring *n* have been based on the principle of the total internal reflection (TIR) on the interface of two media. There are also some other practical techniques for direct and indirect measurements of *n* (goniometry, ellipsometry, interferometry, frustrated TIR, see, e.g. [1, 5-8]), however, most of them require averaging over a large macroscopic volume of the sample. As a result the question of the local fluctuations of *n* in real solids remains unanswered. Moreover, in view of the growing interest to nanotechnology and nanophotonics, it is important to know whether there is a relation between *n* and micro- and nanoscopic structure of solids. In order to give the answer some special instruments for probing the local *n* values on the sub-wavelenght (nanometer) level must be developed.

The topical papers describe a great number of very promising "nanoinstruments" for probing of various local parameters of a sample based on single quantum light emitters embedded into the sample's material. For example, single-molecule (SM), single quantum dot (QD) and single nanocrystals spectroscopy and imaging provides an outstanding basis for various kind of nanoinstrumentation, like nanoscale thermometry [9], nanodetectors of acoustic strain [10], single charges detectors [11], instruments for probing of low-energy excitations in disordered solids [12-17], etc. Besides, we see a possibility to use SM spectroscopy for probing the local-field effects in dye-doped solids. It is well know that the local-field effects cause the dependence of the exited state lifetime of a light emitter on the refractive index of the hosting medium $T_1(n)$ [18-25]. Thus, the study of photo-physical properties of a single dye center is the way to probe the local *n* values. For example, in [26] such an idea was realised by analysing the fluorescence decay of QDs.

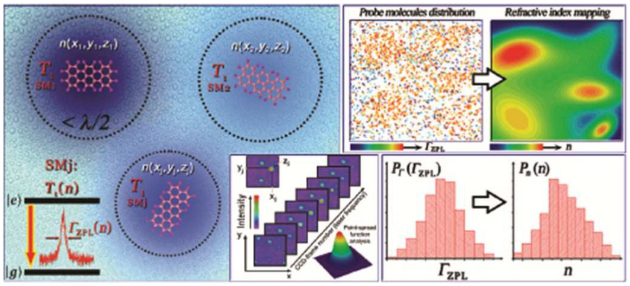

Figure 1. The illustrative sketch of the developed approach for the probing of local values of the refractive index *n* in solids.

In this work we propose a method for the probing of the local (nm-scale) fluctuations of *n* in solids by the analysis of zero-phonon spectral lines (ZPL) of single impurity dye-molecules at ultra-low temperatures (Fig. 1).

---

[a] Molecular Spectroscopy Dept., Institute for Spectroscopy of the Russian Academy of Sciences. Troitsk Moscow, 142190 Russia. Web-page: www.single-molecule.ru. E mail: a_v_naumov@mail.ru. Phone: +7(495)8510236; Fax: +7(495)8510886.

[b] Chair of the Theoretical Physics, Institute of Physics, Technology and Information Systems, Moscow State Pedagogical University. Moscow, 119991, Russia.

* Corresponding author: Prof. Dr. Andrei V. Naumov, E-mail: a_v_naumov@mail.ru

2. Theoretical

The possibility to measure the index of refraction on the sub-wavelength scale is extremely important because of the explosive growth of interest to nanophotonics and related fields. The refractive index *n* is taken into account in all model calculations and theoretical analysis (e.g. development of single-photon sources, hybrid nanostructures, nanodevices, nanoscale metamaterials), but scientists usually consider just the average *n* value for the specific material. At the same time, the local *n* values in a macroscopically homogeneous material can be distributed in a very broad range for the different microscopic volumes. This fact should be obviously taken into account in any nanophotonics applications.

ZPL, which corresponds to a purely electronic transition in an impurity molecule [27], is a unique source of information about dye-matrix interactions [12, 13]. ZPL parameters (frequency, intensity, width, etc.) are very sensitive to the local environment of the corresponding chromophore SM. This fact makes SMs good candidates for spectral probes to obtain data on the structure and the internal dynamics of solids.

As we know from numerous studies, the temperature *T* dependence of the homogeneous spectral width of ZPL is determined by three main contributions[12-16], i.e.

$$\Gamma_{\mathrm{ZPL}}(T) = \Gamma_0 + \Delta\Gamma_{\mathrm{e-tunn}}(T, t_m) + \Delta\Gamma_{\mathrm{e-phon}}(T), \tag{1}$$

where the natural (lifetime limited) linewidth Γ_0 is

$$\Gamma_0 = \frac{1}{2\pi T_1}; \tag{2}$$

the ZPL broadening due to the interaction of electronic transitions in impurity molecules with tunneling excitations in a matrix is

$$\Delta\Gamma_{\mathrm{e-tunn}}(T, t_m) \sim T^{\alpha}\ln(t_m); \tag{3}$$

the ZPL broadening due to the quadratic electron- phonon interaction, which in the simplest case of interaction with a single quasilocalized low-frequency vibrational mode (LFM) is expressed as

$$\Delta\Gamma_{\mathrm{e-phon}}(T) = w\frac{\exp(-\Delta E/kT)}{[1-\exp(-\Delta E/kT)]^2}; \tag{4}$$

In these equations t_m is the total time of measurement, $1 \le \alpha < 2$ and its exact value depends on the dye-matrix system, *w is* the constant of quadratic electron-phonon coupling, ΔE is the energy of LFM.

ZPL width is also a function of the laser excitation intensity P_{LAS} :

$$\Gamma_{\mathrm{ZPL}}(P_{LAS}) = \Gamma_{\mathrm{ZPL}}(0)\sqrt{1 + \frac{P_{LAS}}{P_S}}, \tag{5}$$

where P_s is the saturation intensity and $\Gamma_{ZPL}(0)$ is the unsaturated ZPL spectral width.

From Eqs.(1-5) it follows that if $P_{LAS} \ll P_S$ and the temperature is in the range of ultra-low values, then the additional broadenings $\Delta\Gamma_{e\text{-}tunn}$ and $\Delta\Gamma_{e\text{-}phon}$ can be neglected and for each SM it is possible to measure the lifetime-limited ZPL spectral width related to T_1. Numerous experiments have shown, that these conditions are achieved at $P_{LAS} < 0.1 - 10.0 \mathrm{W{\cdot}cm^{-2}}$ and at T<1-5K (depending on the type of the matrix, see e.g. [28, 29]). Thus, SMs can be used as very sensitive probes of T_1 fluctuations due to the local-field effects.

As a primary step, the light emitters can be viewed as if they are (quasi)homogeneously distributed over some macroscopic space while the space that separates their localities is an *n*-valued “continuous medium”. We assume that this *n* is the averaged value and there are variations of the effective index in the regions that contain a single emitter (due to local matrix inhomogeneities). In reality, a specific host material may require a more accurate theory because of numerous types of complexity. The local environments around an emitter can be of its own *n* value contrasting with the bulk host matrix or be a discrete or structured region where the continuous medium approximation is not applicable. If we leave these cases for a later discussion in this section (e.g., recent[30-32]), the correction factors for T_1 can be summarized using five models [20-24]. They all consider the situation when a guest molecule emits light to the continuous medium of the host matrix, that is weakly absorbing, isotropic and characterized by *n*. Most generally, the effective T_1 is written as[19, 20]:

$$T_1(n) = \frac{\tau_0}{n f(n)}, \tag{6}$$

where τ_0 is the “vacuum” value of the excited state lifetime; *n* is the refractive index (if precisely, at the wavelength of the emitted light); function *f*(*n*) reflects the local-field contributions and includes either squared or straight *n*-dependent coefficient *l*(*n*) being the proportionality between the local-field acting on the emitter E_L and the average Maxwellian field E_M, i.e., $E_L = l(n)E_M$.

To this date, the choice of *l*(*n*) has been among two concepts of the local-field. One is the Lorentz local-field which is classically calculated under the assumption that the field due to polarized molecules inside a small sphere centered at the site of a light emitter may be neglected. The other is a simplified variant of Onsager’s approach, [33] where there is a small empty cavity around the emitter. These cases are often distinguished by the concept of interstitial and substitutional guest molecules [25]. The most popular models for the lifetime correction are the virtual-cavity model [21, 22] based, respectively, on the Lorentz local-field:

$$f(n) = \left(\frac{n^2+2}{3}\right)^2, \tag{7}$$

and the real- or empty-cavity model [23] based on the Onsager model for the local-field:

$$f(n) = \left(\frac{3n^2}{2n^2+1}\right)^2. \tag{8}$$

Another approach is called the fully microscopic model [24], in which

$$f(n) = \frac{1}{n}\left(\frac{n^2+2}{3}\right). \quad (9)$$

Similar to Eq. (7) it uses the Lorentz field but here the *l*(*n*) function is not squared. At the same time it misses the *n* factor in the final form of (6). The remaining models imply *f*(*n*) = *l*(*n*) [20] which brings back the missing *n* and provides agreement with the fully microscopic model (9) in terms that the local-field coefficients *l(n)* are not squared. Thus, for the likely-to-be-interstitial emitters:

$$f(n) = \frac{n^2+2}{3}, \quad (10)$$

while for the likely-to-be-substitutional emitters:

$$f(n) = \frac{3n^2}{2n^2+1}. \quad (11)$$

Speaking generally, the models in Eqs. (7) and (8) are based on the field quantization procedures in dielectrics and other macroscopic concepts for treating the problem of spontaneous emission. The models in Eqs. (9)-(11) appeared from derivation of the Maxwell-Bloch equations describing the light-matter interaction using the Heisenberg operator formalism for (9) and Bogoliubov-Born-Green-Kirkwood-Yvon equations for reduced density matrices and correlation operators of material particles and modes of the quantized radiation field for (10)-(11). In both approaches the field operators were initially written for material vacuum providing interactions between the guest and host particles.

Nevertheless, each of these models (7)-(11) has found "verification" during the analyses of the experimental data [19, 20]. In all cases the so-called vacuum excitation lifetime τ_0 was subjected to variation during the fitting procedure. Depending on the model used for data fitting, for each emitting system the preferable $T_1(n)$ dependence was obtained. It must be noted, however, that the verifications of the models were based on the data from the excited state lifetime measurements for dopants in crystals and glasses as well as quantum dots in various solutions. It has never been performed for such impurity systems as organic molecules in solid matrices with different degree of disorder and, specifically, has never been tried on SMs. Here we make the first attempt to test this approach using several sets of unique data obtained by different research groups.

Returning to the models that describe specific materials and systems and, consequently, include a greater number of parameters, we note that in Refs. 30, 32, 34 they, as well, agree with writing the concept (6)-(8) as a starting point. Now some sophistications are the following. In Ref. 32 they study the decay dynamics of ions in nanocrystals in various solvents with different *n*. A more appropriate model for their case was shown to be

$$f(n) = \left(\frac{3n^2}{2n^2+n_{NC}}\right)^2 [1 + f(n, n_{NC}, \alpha)] \quad (12)$$

where, if compared to (8), the unit in the denominator (being actually the index of the empty cavity) is substituted with the refractive index of the nanocrystal n_{NC}, the term in the square brackets describes the second-order correction including the its radius [35], and n the index of the solvent.

In the studies of polymers using the SM lifetime fluctuations [34], they used

$$f(n) = \left|\frac{\mu_{tot}}{\mu}\right|^2 \left(\frac{n^2+2}{3}\right)^2, \quad (13)$$

as the final working formula. Here, the difference to (7) is the factor in the right hand side. This factor follows from the ~~polymers~~ structure theory. It is the ratio between the total dipole μ_{tot} in the cavity and the dipole μ associated with the charge distribution of the probe molecule and is calculated numerically. It must be noted that the simulated lifetime distributions for this case are strongly dependent on this ratio in terms of broadening and asymmetry. This behavior of distributions was shown to be in good agreement with the one experimentally observed in Refs. [34, 36] where SM lifetime fluctuations were used to reveal the segmental dynamics in polymers at room and higher temperatures.

The calculations of the spontaneous decay of an exited atom in a dense atomic cloud were performed numerically for the model when the continuous medium approximation does not apply. [31] It was shown that direct calculations give different results from the *n*-value concept for both the similar and a foreign atom cases.

3. Experimental results and methods

In this work we have chosen terrylene (Tr) [37] as the object of analysis. It has been widely studied in different matrixes by the laser selective spectroscopy methods, and is one of the most used fluorophores in SMS. For this compound the T_1 values were measured for a set of solid matrices [38]: *polyethylene* (PE), *polystyrene* (PS), *polyvinyl-butyral* (PVB), *polymethyl-methacrylate* (PMMA), and solid *n-hexadecane* (Hex). In the context of the present work we also had to find the refractive indices for these matrices. The *n* values for PE, PS, PVB were found in [39], whereas PMMA and HEX refractive indexes were measured by our team using the laboratory Abbe refractometer (see the table in Fig.2).

A. Refractive index measurements

To obtain the refractive indices of different polymer matrices as well as of liquid solutions the laboratory Abbe refractometer URL-1 was used. The measurements were performed at the temperature 20 ± 0.1 °C.

a) In the case of liquids a drop of the solution under study was placed between the faces of the illuminating and the measuring prisms.

b) In the case of solids optically uniform sample should have two mutually perpendicular polished planes, one of which must be equal in size to the entrance face of the measuring prism. The sample under study was placed on the entrance face of the measuring prism. To achieve a good optical contact an immersion oil was used. The second polished plane of the sample was facing towards the refractometer illuminator.

c) During the measurements the critical angle of the total internal reflection on the sample/prism interface was obtained and the sample refractive index *n* value was found.

B. Excited state lifetime measurements in bulk dye-doped sample

The values of terrylene fluorescence lifetimes in different matrices were obtained in [38] by measuring fluorescence decays excited by picosecond pulses of Nd:YAG laser and recorded using time-correlated single photon counting followed by specific data analysis.

C. Lifetime-limited single-molecule ZPL widths measurements

The spectra of single terrylene molecules in a naphthalene crystal and in polyethylene have been measured in a custom built by Oxford instruments ^{3}He/^{4}He dilution refrigerator at 30 mK using the fluorescence excitation technique and single-molecule microscopy [37, 38]. Each registered SM ZPL was then fit with Lorentzian function, thus the values of SM linewidths were obtained. The power broadening of SM spectra was taking into account and the proper corrections of SM linewidths values were performed (see details in [37, 38]).

D. Materials and samples under study

Terrylene (Tr) is a fluorescent molecule which belongs to the family of rylene dyes, which are extremely persistent against photo-bleaching and characterized by weaker blinking (as compared to other types of fluorophores) in a broad range of temperatures. Tr is characterized by strong absorption, high fluorescence quantum yield, negligible population of triplet states, weak electronphonon coupling at low temperatures, and high photo-stability.

Samples for excited state lifetime measurements were prepared by combining 0.1 to 1 μM solutions of the terrylene dissolved in dichloromethane into about a 0.1% (w/w) solution of the polymers and or semi-crystalline forming solids. The hosts utilized were polyvinyl- butral, polymethyl-methacrylate, polystyrene, and hexadecane. Approximately 12 μL of the combination was transferred via a micropipet onto quartz cover glasses where the drop size averaged about 5 mm in diameter. All samples were baked for evaporation of the solvent and for structural stability. The standard sample thickness was about 1 to 5 mm (see details in [38]). The preparation of samples for lifetime-limited ZPL widths measurements was the following:

a) Mixed crystals of terrylene in naphthalene were prepared by co-sublimation under a nitrogen atmosphere, which produced thin crystals with excellent optical quality. A single crystal was used as a sample, which had a thickness of 10 μm and a diameter of 1 mm. The concentration of terrylene molecules was 10^{-8} M (see details in [40])

b) The sample was prepared by means of diffusion, by heating a small amount of terrylene together with some polyethylene at 180 °C under vacuum for several hours. A small amount of the hot mixture was pressed between two polished stainless steel flats to produce a 2 μm thick film. To avoid surface broadening, the doped film was then melted between two undoped PE films, so that no SM was within 10 μm from the sample surface. (see details in [41]).

E. Analysis of experimental data

In Fig. 2 we have plotted the T_1 values for Tr molecules in all of the above mentioned matrixes against the values of *n* in these systems. The $T_1(n)$ experimental dependencies were fitted using different models (Eqs. 7-11) of the local-field correction factors including the virtual-cavity model [21, 22], the real- or empty-cavity model [23] the fully microscopic model [24], and the two models from a quantum-kinetic approach for derivation of the effective Maxwell-Bloch equations [20].

4. Results and discussions

The best fit was proved to correspond to the virtual-cavity model Eq. 7 (red curve in Fig.2, with the value of τ_0= 12.1 ns (i.e., Γ_0 = 13.1 MHz).

Given the value τ_0 and the best dependence $T_1(n)$ for the Tr molecule, we can calculate the local value of *n* at the position of a SM from its lifetime-limited ZPL width measured in the matrix involved (Fig. 1. To do this, we have taken the unique experimental data on SM ZPL width distributions form Refs. obtained in the ETH, Zurich (inset in Fig. 3 [37, 38]. The authors had performed unprecedented and complicated measurements at milliKelvin temperatures on the SMS setup equipped with the ^{3}He/^{4}He dilution cryostat. At these conditions, the broadening contributions $\Delta\Gamma_{e\text{-}tunn}$ and $\Delta\Gamma_{e\text{-}phon}$ were negligible. The measurements were performed at the laser excitation intensities well below the saturation intensity. Thus, in accordance with Eq. 5 the obtained data were the distributions of lifetime-limited SM ZPL widths Γ_0 directly related to SM effective excited state lifetimes T_1.

These distributions $P_{\Gamma o}(\Gamma_0)$ can be easily converted into the distributions of $P_{T1}(T_1)$ using Eq. 2. Afterwards distributions of $P_{T1}(T_1)$ can be transformed into the distributions of refraction indices $P_n(n)$ by numerical solving of corresponding equations (7-11 with core Eq. 6). For example Fig. 3 demonstrates the result of such conversions with the virtual-cavity model (Eq.7, τ_0 = 12.1 ns), the empty-cavity model (Eq.8) and the microscopic model (Eq. 10)

Considering these distributions of *n* obtained for the polycrystalline and the polymer media one should note the following: (a) there are significant fluctuations of the refractive index local values in real materials; (b) the value of *n* measured in a bulk sample by classical methods corresponds to the peak of the $P_n(n)$ obtained in the sample. Fig. 3 shows that this is valid for polyethylene and naphthalene. This implies the applicability of the proposed approach for the probing of the local fluctuations of the refractive index; (c) the local fluctuations of *n* in the amorphous polymer are substantially greater than in the molecular polycrystal.

One can note that the experimental data points of the initial dependence $T_1(n)$ lie in the region of *n*-values (1.4-1.6) which is narrower than the found region of n-values distributions $P_n(n)$. It means, in principle, that for a broader range of n another model may be more appropriate (or even a new model should be developed). In order to answer this question, the experimental data for $T_1(n)$ for a broader range of n should be obtained.

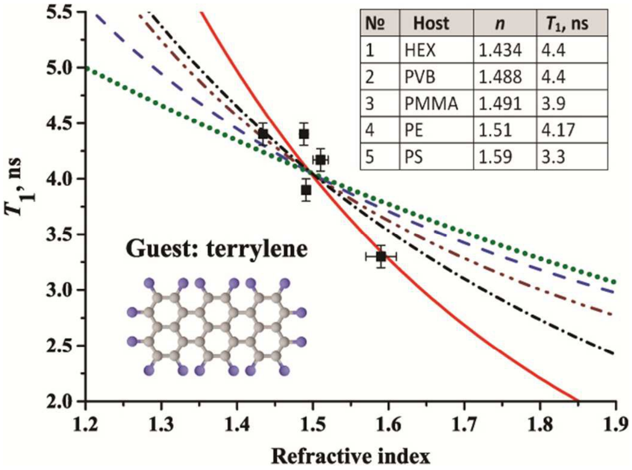

№	Host	n	T_1, ns
1	HEX	1.434	4.4
2	PVB	1.488	4.4
3	PMMA	1.491	3.9
4	PE	1.51	4.17
5	PS	1.59	3.3

Figure 2. The dependence of the excited state lifetime $T_1(n)$ of terrylene on the refractive index of its host matrix (squares). The curves show the best fits of the $T_1(n)$ dependence using different models: the virtual-cavity model (red solid); the empty-cavity model (brown dash-dot-dot); the fully microscopic models (green dot); microscopic model in Eq. (10) (black dash-dot) and in Eq. (11) (blue dashed).

If one looks again at Fig. 2, another satisfactory fit is seen (black dash-dot curve), which corresponds to microscopic model (Eq. 10). Note that it includes the Lorentz local-field factor as in the best fit with Eq. 7. The other three models result in much worse approximations. Yet, we have recalculated the distribution of lifetime-limited Γ_0 in naphthalene into the distributions of refraction indices $P_n(n)$ using all the rest models. Fig. 3 shows that the distributions using the fits for Eqs. 10 and 8 are subjected to significant broadening and, what is most important, their peaks are notably shifted from the value of n in bulk naphthalene. The other two $P_n(n)$ distributions not shown are even worse. We treat this as another evidence of the correct choice of the model and the validity of the developed approach. Note that naphthalene was absent among the systems (Fig. 2), in which T_1 was directly measured.

It is necessary to note that for some materials the proposed method can be realized at liquid ^{4}He temperatures (1.5 K and higher). For example, in Ref. [42] it was shown that the measurement of unsaturated ZPL widths Γ_0 of Tr molecules in ortho-dichlorobenzene at T=1.5 K gives the distribution of lifetime-limited spectral width values (see vertical sticks on the inset of Fig. 3). The similar result was obtained in Ref. [29] for para-dichlorobezene doped with Tr. It is important for the prospective applications of the developed method that quite simple ^{4}He based cryostats can be used for nanoscale mapping of local n values instead of complicated ^{3}He cryogenic technique.

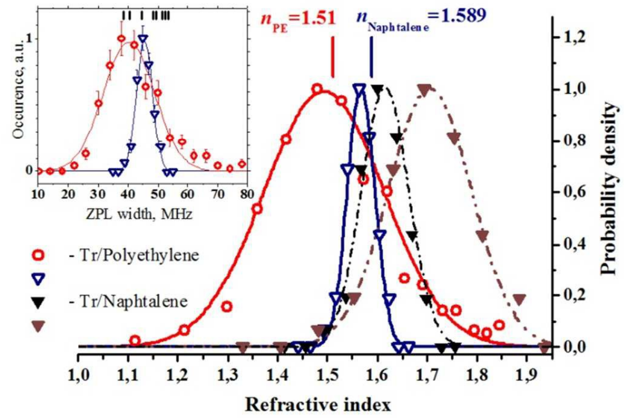

Figure 3. The distribution of the local values of the refractive index in amorphous polyethylene (red circles) and polycrystalline naphthalene (blue triangles). The data are normalized to the maximum value. The sticks mark the average (for bulk media) values of the refractive index of polyethylene (red) [39] and naphthalene (blue) [43]. Black and brown triangles describe the distributions in naphthalene using the satisfactory fit (Eq. (10)) and the fit with Eq. (8). The inset shows the spectral linewidth distribution for terrylene SMs in polyethylene at 30 mK with Gaussian fit of the data [41]. The same for Tr in naphthalene crystal. [40]

Conclusions

To conclude, in our study we propose a unique approach for the probing of the local refractive index fluctuations in solids. The method is based on the detection of SM ZPLs at conditions allowing lifetime-limited spectral line widths. The potential of this approach is demonstrated. Particularly, simultaneous reconstruction of SM spatial coordinates with the nanometre accuracy by super-resolution fluorescence microscopy [44] opens the way to perform sub-wavelength refractometry. In the most advanced version the probing of the local refractive index values in solids can be performed in all 3 dimensions using any 3D luminescence microscopy technique (e.g. double helix point spread function [44, 45]). It was found that there are significant fluctuations of the local n values in amorphous polymer and molecular polycrystalline media. These fluctuations are substantially greater in more disordered medium. The peak of the distribution $P_n(n)$ corresponds to the value of n, averaged over the bulk sample, which is usually obtained by traditional methods.

Acknowledgements

The authors acknowledge support from the Russian Foundation for Basic Researches (project # 14-29-07270).

Notes and references

1. B. V. Ioffe, *Russian Chemical Reviews*, 1960, **29**, 53-66.
2. S. Foteinopoulou, E. N. Economou and C. M. Soukoulis, *Phys. Rev. Lett.*, 2003, **90**.
3. J. Kastel, M. Fleischhauer and G. Juzeliunas, *Physical Review A*, 2007, **76**, Artn 062509.
4. E. Abbe, *Neue Apparate zur Bestimmung des Brechungs – und Zerstreuungsvermögens fester und fluüssiger Körper.*, Mauke's Verlag, Jena, 1874.
5. J. E. Chamberlain, H. A. Gebbie and J. E. Gibbs, *Nature*, 1963, **198**, 874-&.
6. K. G. Muller, S. Sainov, S. MittlerNeher and W. Knoll, *Appl. Optics*, 1996, **35**, 708-710.
7. A. Y. Nassif, *Appl. Optics*, 1997, **36**, 779-785.
8. A. V. Zvyagin, K. Silva, S. A. Alexandrov, T. R. Hillman, J. J. Armstrong, T. Tsuzuki and D. D. Sampson, *Opt. Express*, 2003, **11**, 3503-3517.
9. G. Kucsko, P. C. Maurer, N. Y. Yao, M. Kubo, H. J. Noh, P. K. Lo, H. Park and M. D. Lukin, *Nature*, 2013, **500**, 54-U71.
10. Y. X. Tian, P. Navarro and M. Orrit, *Phys. Rev. Lett.*, 2014, **113**.
11. S. Faez, S. J. van der Molen and M. Orrit, *Phys. Rev. B*, 2014, **90**.
12. T. Basché, W. E. Moerner, M. Orrit and U. P. Wild, *Single-molecule optical detection, imaging and spectroscopy*, VCH, Weinheim ; Cambridge, 1997.
13. A. V. Naumov, *Phys. Usp.*, 2013, **56**, 605-622.
14. I. Osad'ko, *Selective Spectroscopy of Single Molecules*, Springer, 2010.
15. E. Geva and J. L. Skinner, *J. Phys. Chem. B*, 1997, **101**, 8920-8932.
16. Y. G. Vainer, A. V. Naumov, M. Bauer and L. Kador, *Phys. Rev. Lett.*, 2006, **97**, 185501.
17. P. Tamarat, A. Maali, B. Lounis and M. Orrit, *J. Phys. Chem. A*, 2000, **104**, 1-16.
18. R. S. Meltzer, S. P. Feofilov, B. Tissue and H. B. Yuan, *Phys. Rev. B*, 1999, **60**, 14012-14015.
19. K. Dolgaleva and R. W. Boyd, *Adv. Opt. Photonics*, 2012, **4**, 1-77.
20. D. V. Kuznetsov, V. K. Roerich and M. G. Gladush, *J. Exp. Theor. Phys.*, 2011, **113**, 647-658.
21. S. M. Barnett, B. Huttner and R. Loudon, *Phys. Rev. Lett.*, 1992, **68**, 3698-3701.
22. M. Fleischhauer, *Physical Review A*, 1999, **60**, 2534-2539.
23. R. J. Glauber and M. Lewenstein, *Physical Review A*, 1991, **43**, 467-491.
24. M. E. Crenshaw, *Physical Review A*, 2008, **78**.
25. P. de Vries and A. Lagendijk, *Phys. Rev. Lett.*, 1998, **81**, 1381-1384.
26. A. Pillonnet, P. Fleury, A. I. Chizhik, A. M. Chizhik, D. Amans, G. Ledoux, F. Kulzer, A. J. Meixner and C. Dujardin, *Opt. Express*, 2012, **20**, 3200-3208.
27. K. K. Rebane, *J. Lumines.*, 2002, **100**, 219-232.
28. T. Plakhotnik, W. E. Moerner, V. Palm and U. P. Wild, *Opt. Commun.*, 1995, **114**, 83-88.
29. P. Navarro, Y. X. Tian, M. van Stee and M. Orrit, *ChemPhysChem*, 2014, **15**, 3032-3039.
30. R. A. L. Vallee, M. Van Der Auweraer, F. C. De Schryver, D. Beljonne and M. Orrit, *ChemPhysChem*, 2005, **6**, 81-91.
31. A. S. Kuraptsev and I. M. Sokolov, *Physical Review A*, 2014, **90**.
32. T. Senden, F. T. Rabouw and A. Meijerink, *ACS Nano*, 2015, **9**, 1801-1808.
33. L. D. Landau, E. M. Lifésic and L. P. Pitaevskij, *Electrodynamics of continuous media*, Second edn., Pergamon Press, Oxford etc., 1984.
34. R. A. L. Vallee, N. Tomczak, G. J. Vancso, L. Kuipers and N. F. van Hulst, *J. Chem. Phys.*, 2005, **122**, 114704.
35. H. T. Dung, L. Knoll and D. G. Welsch, *Physical Review A*, 2000, **62**.
36. R. A. L. Vallee, N. Tomczak, L. Kuipers, G. J. Vancso and N. F. van Hulst, *Phys. Rev. Lett.*, 2003, **91**.
37. A. Bohnen, K. H. Koch, W. Luttke and K. Mullen, *Angew. Chem.-Int. Edit. Engl.*, 1990, **29**, 525-527.
38. G. S. Harms, T. Irngartinger, D. Reiss, A. Renn and U. P. Wild, *Chem. Phys. Lett.*, 1999, **313**, 533-538.
39. *USA Pat.*, 4,310,584, 1982.
40. E. A. Donley, V. Burzomato, U. P. Wild and T. Plakhotnik, *J. Lumines.*, 1999, **83-4**, 255-259.
41. E. A. Donley, S. Bonsma, V. Palm, V. Burzomato, U. P. Wild and T. Plakhotnik, *J. Lumines.*, 2000, **87-9**, 109-114.
42. A. A. Gorshelev, A. V. Naumov, I. Y. Eremchev, Y. G. Vainer, L. Kador and J. Koehler, *ChemPhysChem*, 2010, **11**, 182-187.
43. D. R. Lide, *CRC Handbook of Chemistry and Physics (90th Edition)*, 90 edn., Boca Raton, Fla. : CRC Press, Florida, 2009.
44. A. Naumov, I. Y. Eremchev and A. A. Gorshelev, *Eur. Phys. J. D*, 2014, **68**, 348.
45. S. R. P. Pavani, M. A. Thompson, J. S. Biteen, S. J. Lord, N. Liu, R. J. Twieg, R. Piestun and W. E. Moerner, *Proc. Natl. Acad. Sci. U. S. A.*, 2009, **106**, 2995-2999.